analytical chemistry

Article

pubs.acs.org/ac

Quantitative Spatial Analysis of the Mouse Brain Lipidome by Pressurized Liquid Extraction Surface Analysis

Reinaldo Almeida,[†] Zane Berzina,[†] Eva C. Arnspang,[§,∥] Jan Baumgart,[‡] Johannes Vogt,[‡] Robert Nitsch,[‡] and Christer S. Ejsing*[,†]

[†]VILLUM Center for Bioanalytical Sciences, Department of Biochemistry and Molecular Biology, University of Southern Denmark, Odense, Denmark

[‡]Institute for Microscopic Anatomy and Neurobiology, Johannes Gutenberg University Mainz, Mainz, Germany

[§]Memphys−Center for Biomembrane Physics, Department of Physics and Chemistry, University of Southern Denmark, Odense, Denmark

Supporting Information

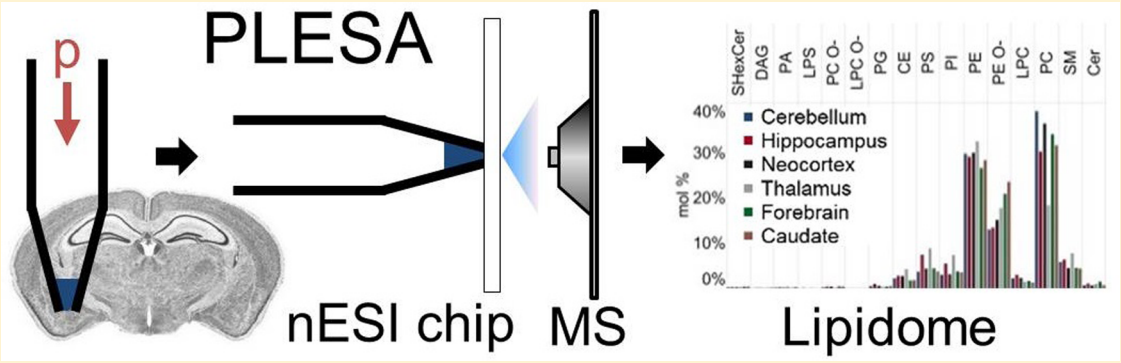

ABSTRACT: Here we describe a novel surface sampling technique termed pressurized liquid extraction surface analysis (PLESA), which in combination with a dedicated high-resolution shotgun lipidomics routine enables both quantification and in-depth structural characterization of molecular lipid species extracted directly from tissue sections. PLESA uses a sealed and pressurized sampling probe that enables the use of chloroform-containing extraction solvents for efficient *in situ* lipid microextraction with a spatial resolution of 400 μm. Quantification of lipid species is achieved by the inclusion of internal lipid standards in the extraction solvent. The analysis of lipid microextracts by nanoelectrospray ionization provides long-lasting ion spray which in conjunction with a hybrid ion trap-orbitrap mass spectrometer enables identification and quantification of molecular lipid species using a method with successive polarity shifting, high-resolution Fourier transform mass spectrometry (FTMS), and fragmentation analysis. We benchmarked the performance of the PLESA approach for in-depth lipidome analysis by comparing it to conventional lipid extraction of excised tissue homogenates and by mapping the spatial distribution and molar abundance of 170 molecular lipid species across different anatomical mouse brain regions.

Lipids comprise a diverse group of molecules with important functions in membrane dynamics, storage of metabolic energy, and signaling.[1] These functions span a wide range of length scales ranging from nanometer-sized lipid rafts controlling intracellular protein sorting and transmembrane signaling events[2] to micrometer-size tissue patterning during development[3] and to the control of tissue mechanical properties and functionality at the centimeter length scale.[4] The regulation of spatial lipid composition and distribution is of paramount importance for mediating lipid functionality and, when disrupted, can promote pathophysiological processes that elicit various disease states including cancer, obesity, atherosclerosis, and neurodegeneration.[5] To improve the understanding of how spatial lipid distribution in tissues impinges on (patho)physiological processes warrants analytical technologies capable of monitoring the full lipid complement (i.e., lipidome) on a variety of length scales.

Lipidomic techniques cover a wide repertoire of mass spectrometry-based workflows affording absolute lipid quantification of several hundred molecular lipid species.[6] These techniques are based on direct infusion mass spectrometry (MS) (i.e., shotgun lipidomics)[7−9] or liquid chromatography (LC)−MS[10,11] using dedicated methods with tandem mass analysis (MS/MS) or high-resolution Fourier transform MS (FTMS) analysis for specific detection of lipid species.[12−14] Notably, these techniques require the use of homogenized sample material and liquid−liquid-based lipid extraction,[12,15−17]

Received: September 27, 2014
Accepted: December 30, 2014
Published: December 30, 2014

DOI: 10.1021/ac503627z
Anal. Chem. 2015, 87, 1749−1756

which disrupts spatial lipid composition and distribution, especially when analyzing tissues. Importantly, when complemented with sophisticated biochemical fractionation strategies these techniques can provide molecular insights at the nanometer and micrometer length scale.[18,19]

Mass spectrometry imaging provides an alternative avenue for profiling lipid distribution at the nanometer and micrometer length scale. Available approaches are commonly based on matrix assisted laser desorption ionization (MALDI),[20,21] secondary ion mass spectrometry (SIMS),[22−24] and desorption electrospray ionization (DESI).[25,26] These approaches allow imaging of lipid species directly from histological tissue sections and correlating the intensity of lipid species with the underlying microscopic anatomy across a variety of tissues including brain,[23,27,28] kidney,[29] lung,[30] and retinal tissue.[31] However, an inherent limitation of mass spectrometry imaging is the hindrance to perform lipid quantification due to ion suppression effects, in-source fragmentation, differential lipid ionization, and difficulties to apply internal standards.[32,33] Moreover, these techniques suffer from limited ion intensities and time for performing in-depth structural analysis and identification of molecular lipid species.

Ambient surface analysis techniques such as liquid extraction surface analysis (LESA) serve as an alternative strategy for spatial mapping of lipid species distribution at the micrometer length scale.[34] LESA is a hyphenated technology that combines robotic sampling of tissue sections with sensitive chip-based direct infusion nanoelectrospray ionization (nESI).[35] The LESA approach analyzes tissue regions by positioning a disposable pipet probe above a tissue section and dispensing an extraction solvent onto it to create a liquid microjunction into which analytes are extracted (Figure 1A). Subsequently, the extraction solvent is aspirated back into the pipet probe and robotically docked onto a nESI chip for direct infusion analysis. The key challenge of the LESA approach is to establish a stable liquid microjunction between the tissue and the pipet probe, which depends primarily on the surface tension and volume of the extraction solvent, the outer diameter of the pipet probe, and the properties of the tissue. LESA has primarily been carried out using water-containing solvents which easily support a stable liquid microjunction with a diameter of more than 1000 μm[35] and as such facilities monitoring the distribution of polar analytes across tissues.[36] In contrast, the LESA approach is of limited efficacy for *in situ* lipid analysis due to the inability to reconcile the use of apolar extraction solvents supporting efficient lipid extraction[15] with the ability to create a stable liquid microjunction due to the low surface tension of apolar solvents. Consequently, spatial analysis of lipids in tissues by LESA uses high extraction solvent volume[37] and yield irregular, uncontrollable, and poor spatial resolution due to solvent spreading across tissue sections (Figure 2B).

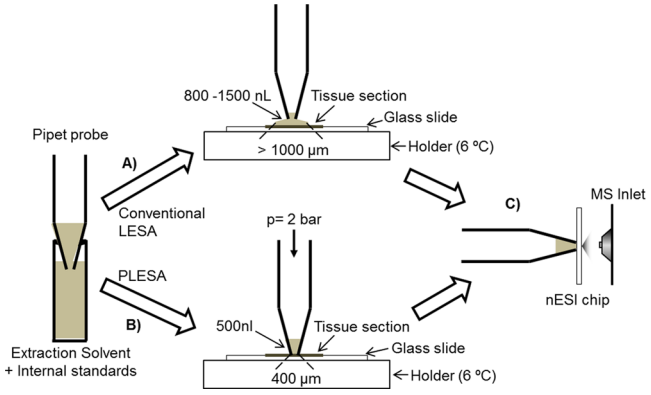

Figure 1. Comparison of conventional LESA and PLESA. Extraction solvent with internal lipid standards is robotically aspirated into a disposable pipet probe. (A) In conventional LESA mode, the pipet probe is positioned above the tissue section to dispense the extraction solvent. Only extraction solvents with high surface tension such as water can sustain a stable liquid microjunction between the pipet probe and tissue surface. Consequently, the spatial resolution of LESA is more than 1000 μm in diameter. (B) In PLESA mode, the pipet probe is pressed onto the tissue section to form a sealed and pressurized microextraction vessel. Headspace pressure is applied to force the extraction solvent onto the tissue. The spatial resolution of PLESA is 400 μm in diameter. (C) After extraction, the pipet probe is moved onto a nESI chip for shotgun lipidomics analysis.

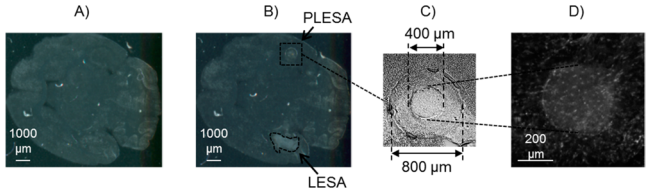

Figure 2. Surface sampling of mouse brain tissue section by conventional LESA and PLESA. (A) Image of a mouse brain tissue section before surface sampling. (B) Image of the mouse brain tissue section after surface sampling by LESA and PLESA. (C) Phase-contrast micrograph of a tissue region sampled by PLESA. The image was recorded using bright field microscopy. (D) Fluorescent microscopy image of a tissue region sampled by PLESA. The spatial resolution of the PLESA is 400 μm.

Here we present a novel surface analysis technique termed pressurized liquid extraction surface analysis (PLESA) which in combination with high resolution shotgun lipidomics analysis enables both lipid quantification and in-depth structural characterization of molecular lipid species extracted directly from tissue sections. This technique was developed to support accurate lipid microextraction at a spatial resolution of 400 μm using a sealed and pressurized pipet probe which allows the use of organic extraction solvents containing internal lipid standards for lipid quantification (Figure 1B). Moreover, the approach uses a low flow rate nESI chip providing stable spray for performing quantitative *in situ* tissue lipidomic analysis using a dedicated shotgun lipidomics method with successive polarity shifting, high-resolution FTMS, and fragmentation analysis for structural characterization of molecular lipid species. To evaluate the performance of the PLESA approach for lipidomics analysis, we compared it to conventional lipid extraction of excised tissue homogenates and by mapping the spatial distribution and molar abundance of 170 molecular lipid species across different anatomical mouse brain regions.

MATERIALS AND METHODS

Annotation of Lipid Species. Lipid species were annotated as previously described.[12,38] In short, glycerophospholipid and glycerolipid species were annotated by either sum composition (e.g., for phosphatidylcholine (PC) species PC 34:1) or by molecular species composition (e.g., PC 16:0-18:1). Sphingolipid species were annotated by sum composition (e.g.,

DOI: 10.1021/ac503627z
Anal. Chem. 2015, 87, 1749−1756

for ceramide (Cer) species Cer 34:1;2) or by molecular species composition (e.g., Cer 18:1;2/16:0;0).

Chemicals and Lipid Standards. Lipid standards were obtained from Avanti Polar Lipids (Alabaster) and Larodan Fine Chemicals (Malmö, Sweden). Ammonium acetate and ammonium formate were from Fluka Analytical (St. Gallen, Switzerland). Chloroform, methanol, and 2-propanol were from Rathburn (Walkerburn, Scotland). All solvents and chemicals were HPLC grade.

Preparation of Mouse Cerebellum and Hippocampus. Animal experiments were conducted in accordance with German law (in congruence with 86/609/EEC) for the use of laboratory animals and approved by the local animal welfare committee at the Johannes Gutenberg University Mainz. Male C57Bl/6 wild-type mice were euthanized by an overdose of ketamine by intraperitoneal injection. Subsequently, the mice were perfused intracardially with cold 155 mM ammonium acetate and the brains were quickly removed and immediately frozen on dry ice and stored at −80 °C. For PLESA, frozen brain tissue was cut into 15 μm thick sections in a cryostat (CM 3050 S; Leica Microsystems, Nussloch, Germany), placed on a glass slide, and stored at −80 °C. For lipid extraction by a modified Bligh and Dyer procedure, cerebellum and hippocampus were dissected, homogenized, and stored at −80 °C until further processing.

Lipid Extraction by a Modified Bligh and Dyer Procedure. Mouse cerebellum and hippocampus homogenates were analyzed for total protein concentration using a BCA Protein Assay Kit (Thermo Fisher Scientific). Lipid extraction was performed at 4 °C using a modified Bligh and Dyer extraction procedure.[39] In short, aliquots of tissue homogenates corresponding to 10 μg of protein were diluted with 155 mM ammonium acetate to 200 μL and spiked with 10 μL internal standard mix containing 19 internal lipid standards (Supporting Information, Table S-1). Subsequently, 990 μL chloroform/methanol (2:1, v/v) was added to the samples, vigorously mixed for 120 min, and centrifuged for 2 min at 1000*g* to promote phase separation. The lower organic phase was collected in a new tube, vacuum evaporated, and dissolved in 100 μL of chloroform/methanol (1:2, v/v) prior to MS analysis.

***In situ* Sampling by PLESA.** Glass slides with 15 μm thick brain tissue sections were placed onto a sample holder and imaged using a flatbed scanner. The image was calibrated for PLESA using LESA Points Software (Advion Biosciences, Ithaca). The sample holder was then placed into a TriVersa NanoMate (Advion Biosciences, Ithaca), and selected tissue regions were analyzed. For PLESA the conventional LESA mode was modified to create a sealed microextraction vessel between the brain tissue section and the extraction solvent (Figure 1B). TriVersa NanoMate tubing connections were modified to enable the application of headspace pressure during the extraction. A volume of 500 nL of extraction solvent with a mix of internal lipid standard in 0.75 mM ammonium formate in chloroform/methanol/2-propanol (1/2/4, v/v/v) was aspirated and applied on the tissue regions for 30 s and subsequently analyzed using a low flow rate nESI chip at a flow of 40−50 nL/min.

Shotgun Lipidomics Analysis. Mass spectrometric analysis was performed using an LTQ Orbitrap XL (Thermo Fisher Scientific, Bremen) equipped with the TriVersa NanoMate. Lipid extracts were analyzed as previously described,[12] whereas tissue sections were analyzed by PLESA. Both sample types were analyzed using polarity shifting with 4.75 min positive and negative ion mode analysis. For lock mass calibration we used the m/z of internal lipid standards (e.g., m/z 778.5381 corresponding to protonated PC 18:3-18:3). FTMS spectra were acquired in profile mode using a target mass resolution of 100 000 (fwhm at m/z 400), with injection waveform activated and automatic gain control set to 1×10^6, and a maximal injection time of 1000 ms. In positive ion mode the scan ranges alternated between m/z 200−700 and m/z 600−1200 and in negative mode between m/z 200−400, m/z 375−675, and m/z 600−1600 to monitor specific lipid classes (Supporting Information, Figure S-1). In addition, data dependent acquisition was used to trigger collision-induced dissociation (CID-ITMS^2) of the 5 (Top 5) or 20 (Top 20) most abundant lipid precursors within each m/z range based on a priori knowledge about the spectral complexity within m/z ranges. The cycle time for the FTMS scans and ITMS^2 routine was approximately 30 s resulting in about 10 cycles for each polarity mode. Dynamic exclusion was used such that each precursor m/z was fragmented only once. ITMS^2 was performed using normalized collision energy of 35%, isolation width of 2 amu, and 2 μscans. Neutral loss activation was used on specific neutral losses (i.e., loss of methylformate from PC formate adducts, loss of serine from phosphatidylserine (PS) species, loss of formate from Cer) to produce more informative MS^2 spectra.[40] The activation Q parameter was set to 0.2 to detect lower mass fragment ions, e.g., phosphocholine at m/z 184.1.

Data Analysis. Lipid species detected by FTMS analysis were identified using ALEX software.[41] The molar abundance of lipid species were calculated using open source software Orange and converted to mol % values and visualized using Tableau software, as previously described.[41]

Imaging of Tissue Sections by Fluorescence Microscopy. Fluorescence microscopy was performed on a Nikon Ti eclipse inverted microscope equipped with a Yokogawa spinning disk unit and an Andor EMCCD camera (model Andor iXon EM+). The tissue sections were stained with Hoechst 33258, and images were acquired using an excitation wavelength of 405 nm with a 500 ms integration time at 4× magnification.

RESULTS AND DISCUSSION

PLESA: a Novel Strategy for *in Situ* Lipid Analysis. Central to the PLESA approach is the ability to accurately extract and determine the lipid composition of distinct tissue regions. To this end, we modified the conventional LESA method (Figure 1A) to allow pressing a disposable sampling pipet probe containing extraction solvent directly onto tissue sections and thereby establish a sealed and pressurized microextraction vessel. Headspace pressure is applied to force the extraction solvent onto the tissue (Figure 1B). As such, the PLESA approach allows using apolar extraction solvents and surface sampling with a consistent spatial resolution of 400 μm in diameter as compared to the irregular and poor spatial resolution obtained by conventional LESA (Figure 2B). For optimal lipid microextraction we positioned the pipet probe with 500 nL of extraction solvent directly onto tissue sections for 30 s. The extraction solvent was 0.75 mM ammonium formate in chloroform/methanol/2-propanol (1/2/4, v/v/v) and contained a mixture of internal lipid standard to support lipid quantification. We note that the lipid extraction efficiency did not improve when extracting for longer than 30 s (data not

DOI: 10.1021/ac503627z
Anal. Chem. 2015, 87, 1749−1756

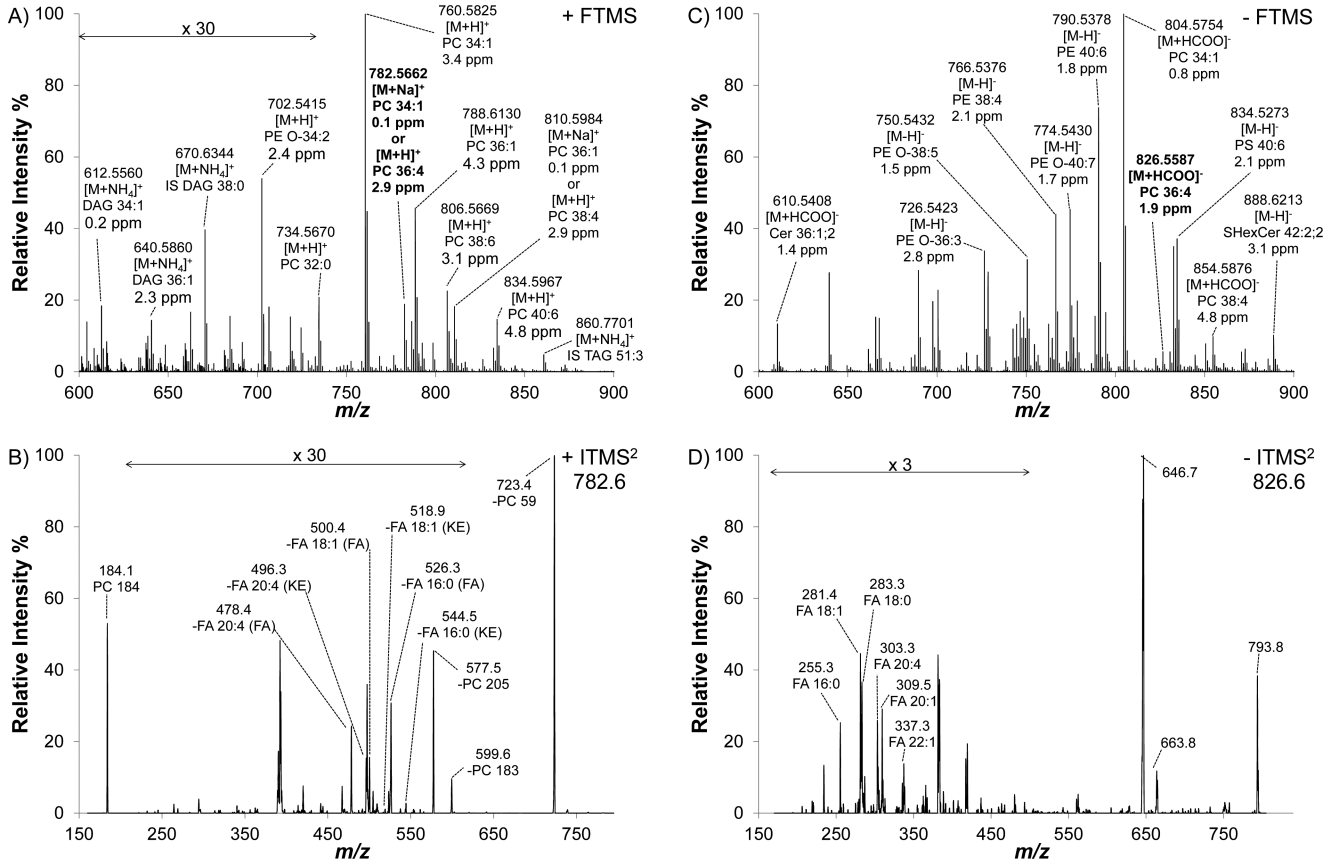

Figure 3. *In situ* lipid analysis of cerebellum by successive positive and negative ion mode FTMS and ITMS^2 analysis. (A) Positive ion mode FTMS spectrum. Identified lipid species are reported with m/z, adduct ion, sum composition, and mass accuracy in ppm. The precursor ion at m/z 782.5662 can be identified as both $[PC\ 34:1 + Na]^+$ and $[PC\ 36:4 + H]^+$. (B) Positive ion mode ITMS^2 spectrum of m/z 782.6. Detection of low abundant fragment ions derived from neutral loss of fatty acid moieties as fatty acids (e.g., −FA 16:0 (FA)) or ketenes (e.g., −FA 16:0 (KE)), and phosphocholine at m/z 184.1 and neutral loss of trimethylamine at m/z 723.4 (−PC 59). Using this information, two isobaric species are identified as sodiated PC 16:0-18:1 and protonated PC 16:0-20:4. (C) Negative ion mode FTMS spectrum. Identified lipid species are reported as in panel A. (D) Negative ion mode ITMS^2 spectrum of m/z 826.6 corresponding to PC 36:4 as a formate adduct. Detection of acyl anions FA 16:0 and FA 20:4 identifies PC 36:4 as the molecular lipid species PC 16:0-20:4.

shown). Importantly, the composition and the volume of the extraction solvent provided stable nESI for more than 10 min, which render ample time for in-depth shotgun lipidomics analysis.

In-Depth Lipidome Analysis by Polarity Shifting, FTMS, and ITMS^2 Analysis. For in-depth shotgun lipidomics analysis, we applied a dedicated method with successive polarity shifting, high-resolution FTMS analysis for lipid quantification, and ITMS^2 analysis for identification of molecular lipid species (Supporting Information, Figure S-1). Using this routine, each tissue region was analyzed in 10 min, where half of the time was spent doing either positive or negative ion mode analysis. The routine allowed acquisition of 8−10 FTMS spectra and 150−250 ITMS^2 spectra per polarity. Notably, this scope of mass spectrometric analyses is not supported by mass spectrometry imaging platforms due to their limited sensitivity and limited time for fragmentation analysis. In order not to compromise the high mass accuracy of high-resolution FTMS analysis due to polarity shifting, we applied online lock mass calibration.[42] Importantly, the use of polarity shifting allows uncompromised lipid ionization and detection specificity, which strongly depends on the acquisition polarity,[12,43] and as such supports optimal detection of lipid species and their structure-specific fragment ions.

As a proof of principle experiment, we deployed the shotgun lipidomics routine in conjunction with PLESA-based lipid microextraction of mouse cerebellum. This experiment demonstrated that the approach could successfully identify (and quantify, see next section) molecular lipid species with mass accuracy at the low parts-per million (ppm) range using positive and negative FTMS analysis and ITMS^2 analysis for mapping structure-specific fragment ions. For example, the species PC 36:4 could be detected with a mass accuracy of 2.9 ppm in positive ion mode ($[M + H]^+$, m/z 782.5662) and 1.9 ppm in negative ion mode ($[M + HCOO]^-$, m/z 826.5587) (Figure 3A,C). ITMS^2 analysis of m/z 782.6 in positive ion mode detected PC-specific fragment ions at m/z 184.1 and m/z 723.4 corresponding to phosphocholine and neutral loss of trimethylamine, respectively (Figure 3B). Moreover, the ITMS^2 analysis also detected fatty acid moiety-specific fragment ions corresponding to the neutral loss of FA 20:4 (m/z 478.4), FA 18:1 (m/z 500.4), and FA 16:0 (m/z 526.3). Notably, this demonstrates the presence of two isobaric lipid species at m/z 782.5662: protonated PC 36:4 and sodiated PC 34:1 with the molecular species compositions PC 16:0-20:4 and PC 16:0-18:1, respectively. Negative ion mode ITMS^2 analysis of PC 36:4 (m/z 826.6) confirmed the identity of PC 16:0-20:4 based on detection of the acyl anions FA 16:0 (m/z 255.3) and FA 20:4 (m/z 303.3), but also detected acyl anions corresponding

DOI: 10.1021/ac503627z
Anal. Chem. 2015, 87, 1749−1756

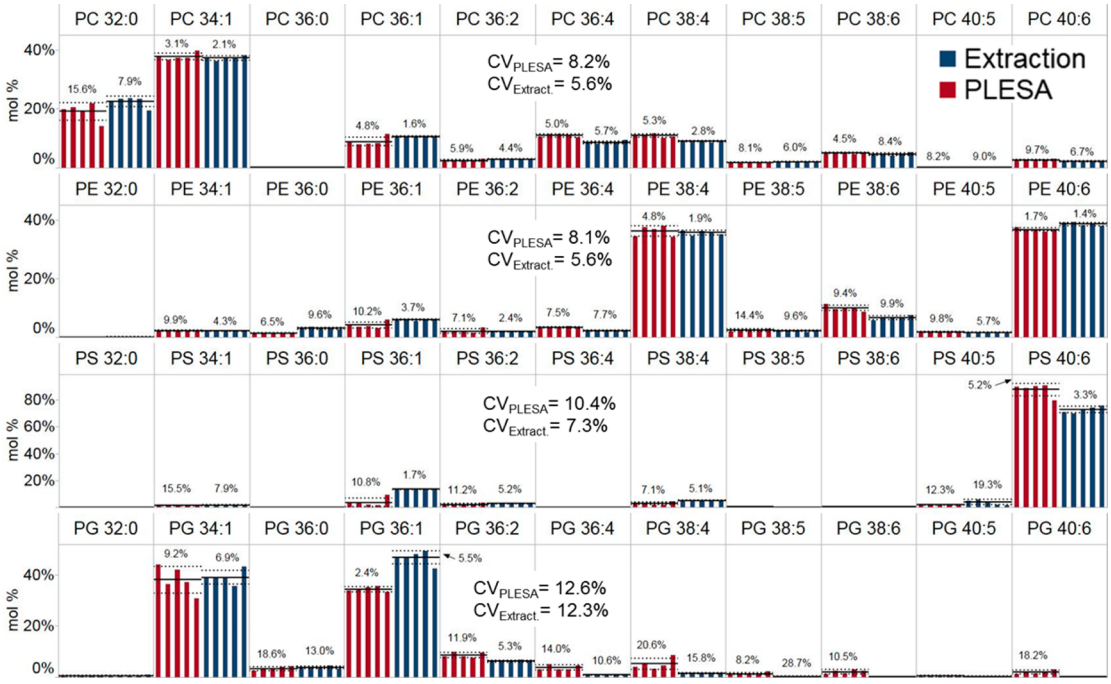

Figure 4. Comparison of lipid profiles determined using conventional lipid extraction of excised and homogenized tissues and PLESA. Molar abundance of glycerophospholipid species determined using lipid extraction of excised and homogenized mouse hippocampus and PLESA microextracts of a hippocampal region. For presentation clarity, only the 44 most abundant lipid species with identical sum composition are displayed for the lipid classes PC, PE, PS, and PG. Lipid extracts of hippocampus were analyzed five times. The hippocampal region by PLESA was analyzed by five consecutive microextractions. Molar abundances were calculated from the FTMS data and are presented as mol % and mean (straight line) ± standard deviation (dotted lines) for $n = 5$. Coefficient of variation (CV) was calculated for PLESA and lipid extraction of the five measurements for each lipid species and as average over the lipid class.

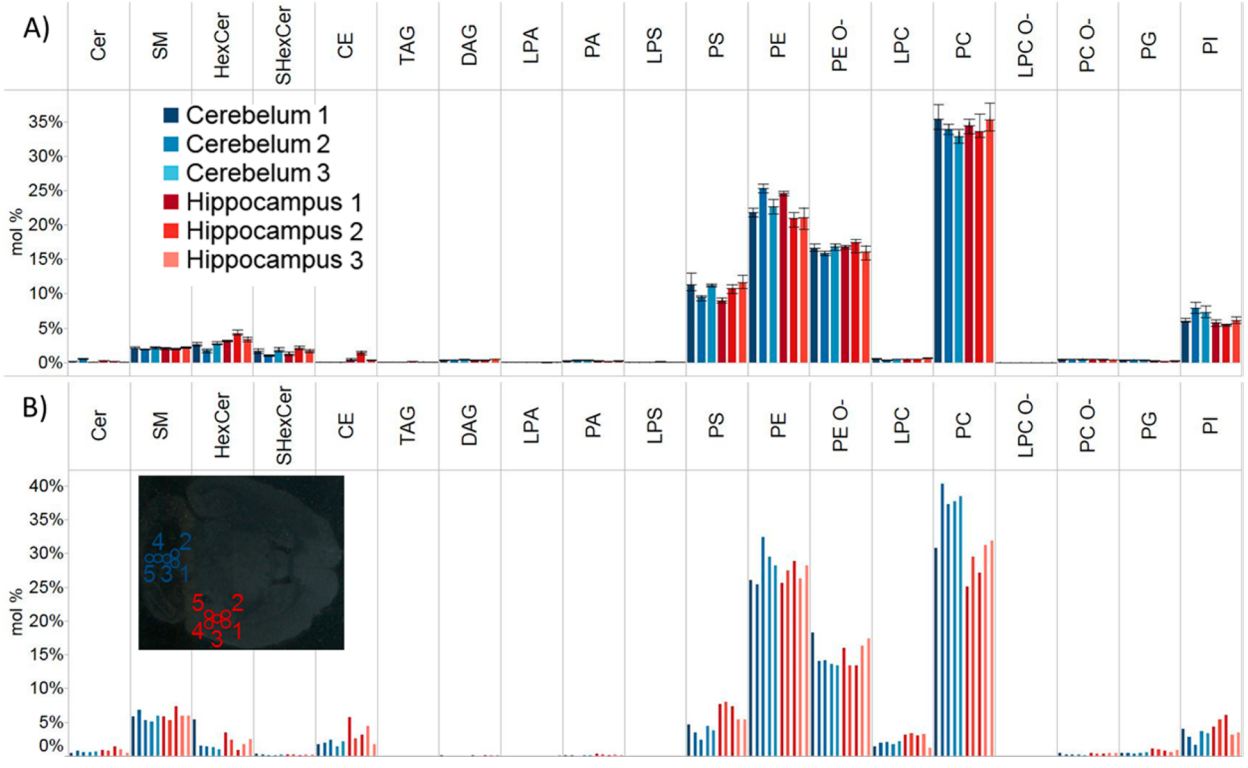

Figure 5. Lipid class composition of cerebellum and hippocampus determined by lipid extraction of tissue homogenates and PLESA microextraction. (A) Lipid class composition determined by lipid extraction of tissue homogenates. Tissue homogenates of cerebellum and hippocampus from three mice were extracted and analyzed applying the shotgun lipidomics routine. Each sample was analyzed in five technical replicates. Error bars show the maximum and minimum molar abundance within the five replicates. (B) Lipid class composition determined using PLESA. A mouse brain tissue section (shown in the insert) was sampled in the cerebellum and the hippocampus at five different regions.

DOI: 10.1021/ac503627z
Anal. Chem. 2015, 87, 1749−1756

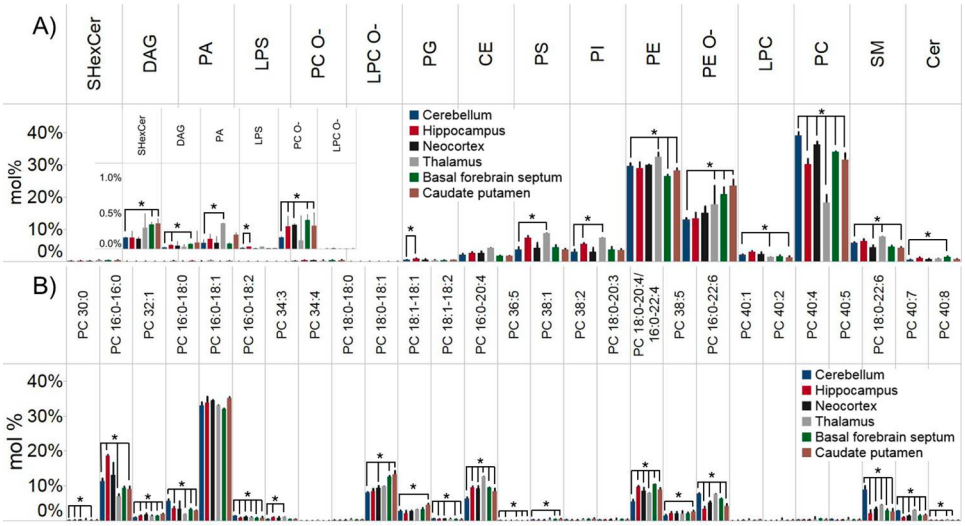

Figure 6. Lipidome composition of mouse brain regions. (A) Lipid class composition of cerebellum, neocortex, basal forebrain septum, caudate putamen, hippocampus, and thalamus determined using PLESA. (B) Composition of molecular PC species. The molar abundances were calculated from the FTMS data and are presented as mol % ± standard deviation for $n = 3$. The statistical comparison of lipid class and PC species levels between the six mouse brain regions was performed with a Student's *t*-test. Differences were considered significant and highlighted with (*) if p values were less than 0.05. Lipid species are annotated by sum composition when identified using FTMS analysis or molecular species composition when identified using $ITMS^2$ analysis and detection of molecular species-specific fragment ions.

to FA 18:1 (m/z 281.4), FA 18:0 (m/z 283.3), FA 20:1 (m/z 309.5), FA 22:1 (m/z 337.3), and glucosylceramide (HexCer)-specific fragment ions at m/z 646.7 and m/z 663.8 indicating the coisolation and fragmentation of PC 16:0-20:4 with HexCer 42:1;3 ($[M - H]^-$, m/z 826.6729) and other lipid species. This demonstrates that high confidence identification requires the combination of FTMS analysis and $ITMS^2$ analysis in positive and negative ion mode as supported by the shotgun lipidomics routine.

On the basis of these and analogous results from other lipids, we conclude that PLESA in conjunction with the dedicated shotgun lipidomics routine is an effective strategy for detection and identification of molecular lipid species *in situ* at a spatial resolution of 400 μm in diameter.

Evaluating the PLESA Approach for Quantitative Lipidome Analysis. To evaluate the technical reproducibility of the PLESA approach for *in situ* tissue lipidomics, we compared the lipid species profile of mouse hippocampus obtained by conventional lipid extraction of excised tissue homogenates and by PLESA of hippocampus. We analyzed the same hippocampal region by five consecutive PLESA micro-extractions and the lipid extracts of hippocampus homogenates applying our shotgun lipidomics routine. To evaluate the reproducibility of the analyses, we compared the molar abundances of 44 glycerophospholipid species with identical sum composition from the lipid classes PC, phosphatidylethanolamine (PE), phosphatidylserine (PS), and phosphatidylglycerol PG (Figure 4). The lipid profiles determined by the two approaches were similar and with good reproducibility demonstrated by low variation between the repeated analyses (e.g., average coefficient of variation (CV) is 9.8% and 7.7% for PLESA and lipid extraction, respectively). Moreover, this evaluation showed that the most abundant glycerophospholipid species in mouse hippocampus are PC 32:0, PC 34:1, PE 38:4, PE 40:6, PS 36:1, PS 40:6, PG 34:1, and PG 36:1. This result is consistent with previous reports on mouse brain lipid composition.[41,44] On the basis of these results, we conclude that PLESA allows reproducible spatial *in situ* lipidome analysis and that lipid profiles match that obtained using conventional lipid extraction of excised tissue homogenates.

Next, we compared the lipid class composition of mouse hippocampus and cerebellum determined using conventional lipid extraction of excised and homogenized tissues (Figure 5A) with that determined by PLESA microextraction of equivalent tissue sections (Figure 5B). These two approaches afforded detection and comparison of 164 lipid species (annotated by sum composition) encompassing 10 lipid classes (Supporting Information, Figure S-3). The lipid class composition determined by PLESA matched closely that obtained by the conventional lipid extraction. Importantly, this result demonstrates that the PLESA approach affords accurate quantification of lipid species *in situ*. The two approaches showed that mouse cerebellum and hippocampus mainly comprise PC, PE, and ether-linked PE (PE O−) lipid species followed by lower levels of PS, phosphatidylinositol (PI), and sphingomyelin (SM) species. As previously observed,[41] we detected no major differences in molar abundance of lipid classes between the mouse cerebellum and hippocampus in homogenized tissues (Figure 5A). In contrast, the *in situ* lipid analysis by PLESA showed subtle differences in lipid class composition within and between the two brain tissues. For example, within the cerebellar region the molar abundance of PE species vary between 26 and 33 mol %. Between the cerebellum and hippocampus, the molar abundance of PC species ranges from 25 to 40 mol %, respectively (Figure 5B). The subtle differences in spatial lipid composition within and between the brain tissues can be attributed to the smaller tissue area sampled by the PLESA approach which is averaged out by the analysis of macroscopic mouse brain tissue homogenates.

Quantitative Spatial Analysis of the Mouse Brain Lipidome. To explore the full potential of the PLESA approach, we executed a comparative *in situ* lipidome analysis of six different mouse brain regions: thalamus, cerebellum, hippocampus, basal forebrain septum, caudate putamen, and neocortex (Figure 6). On the basis of accurate mass FTMS analysis, we identified and quantified 170 lipid species

DOI: 10.1021/ac503627z
Anal. Chem. 2015, 87, 1749−1756

encompassing 11 different lipid classes. On the basis of ITMS^2 analyses, we could define the specific acyl chain composition for 45 molecular lipid species (Supporting Information, Table S-2). The analysis demonstrated that the most abundant lipid class in all brain regions was PC, ranging from 20 mol % in the thalamus to 43 mol % in the cerebellum (Figure 6A). In addition, PE and PE O− were observed to be the second and third most abundant lipid classes in all the surveyed brain regions. Notably, the caudate putamen and the basal forebrain septum display a higher abundance of PE O− (17 and 21 mol %, respectively) compared to all other brain regions. Less abundant glycerophospholipid classes in the brain tissues include PI and PS which are most abundant in the thalamus (7 and 9 mol %, respectively). The most abundant sphingolipid class in all brain tissues was SM ranging from 2 mol % in the caudate putamen to 6 mol % in the hippocampus followed by less abundant sulfatide (SHexCer) and Cer lipids (Figure 6A).

On the molecular species level, PC 16:0-18:1 is the most abundant PC species in all analyzed brain regions (on average 33 mol %) followed by PC 16:0-16:0, PC 18:0-18:1, PC 16:0-20:4, and PC 18:0-20:4 (Figure 6B). Notably, the level of PC 18:0-22:6 is exceptionally high in the cerebellum whereas in the hippocampus PC 16:0-16:0 is more abundant compared to all other analyzed brain regions. The composition of molecular lipid species from other classes can be found in the Supporting Information (Figure S-4). On the basis of our results presented above, we conclude that PLESA combined with shotgun lipidomic analysis is a powerful strategy for comprehensive *in situ* lipidome analysis at a spatial resolution of 400 μm.

CONCLUSION

Here we described a novel *in situ* lipid analysis strategy, termed PLESA, which in combination with a dedicated shotgun lipidomics routine enables both quantitative analysis and structural characterization of molecular lipid species directly from tissue sections at a spatial resolution of 400 μm. The PLESA approach uses a disposable pipet probe with extraction solvent, which is robotically pressed onto the tissue section to establish a sealed and pressurized microextraction vessel. The extraction solvent contains chloroform for efficient lipid microextraction and a cocktail of internal lipid standards for *in situ* lipid quantification. Subsequent chip-based nESI provides long-lasting ion spray for in-depth lipidome analysis by a dedicated shotgun lipidomics method designed to employ polarity shifting for successive positive and negative ion mode high-resolution FTMS analysis supporting accurate lipid quantification and in-depth ITMS^2 fragmentation analysis for identification of molecular lipid species. We demonstrated the efficacy of this novel approach by benchmarking its performance against conventional liquid−liquid-based extraction of lipids and by performing a comparative *in situ* lipidome analysis with absolute quantification of 170 lipid species across six anatomically distinct mouse brain regions. We note that the PLESA approach developed herein is a generic surface sampling technology applicable for quantitative spatial analysis of other biomolecules and other biological tissues.

ASSOCIATED CONTENT

Supporting Information

Additional material as described in the text. This material is available free of charge via the Internet at http://pubs.acs.org.

AUTHOR INFORMATION

Corresponding Author

*Phone: +45 6550 2424. Fax: +45 6550 2467. E-mail: cse@bmb.sdu.dk.

Present Address

‖E.C.A.: Department of Molecular Biology and Genetics, and Interdisciplinary Nanoscience Center (iNANO), Aarhus University, Aarhus, Denmark.

Notes

The authors declare no competing financial interest.

ACKNOWLEDGMENTS

We are grateful to Ole N. Jensen for providing access to the TriVersa NanoMate. We thank the Danish Molecular Biomedical Imaging Center (DaMBIC) and Christoffer Lagerholm for the imaging of tissue sections by fluorescence microscopy. We thank Albert Casanovas and Martin Hermansson for critical reading of the manuscript and constructive comments. We thank Hans Kristian Hannibal-Bach and Nikolai Schmarowski for technical assistance. This work was supported by Lundbeckfonden (Grant R54-A5858).

REFERENCES

(1) van Meer, G. *EMBO J.* **2005**, *24*, 3159−3165.
(2) Lingwood, D.; Simons, K. *Science (New York, N.Y.)* **2010**, *327*, 46−50.
(3) Panáková, D.; Sprong, H.; Marois, E.; Thiele, C.; Eaton, S. *Nature* **2005**, *435*, 58−65.
(4) Fung, Y.-C. *Biomechanics*, 2 ed.; Springer: New York, 1993; Vol. 9, pp 155−155.
(5) Wymann, M. P.; Schneiter, R. *Nat. Rev. Mol. Cell Biol.* **2008**, *9*, 162−176.
(6) Tarasov, K.; Stefanko, A.; Casanovas, A.; Surma, M. a.; Berzina, Z.; Hannibal-Bach, H. K.; Ekroos, K.; Ejsing, C. S. *Mol. BioSyst.* **2014**, *10*, 1364−1376.
(7) Han, X.; Yang, K.; Gross, R. W. *Mass Spectrom. Rev.* **2012**, *31*, 134−178.
(8) Harkewicz, R.; Dennis, E. A. *Annu. Rev. Biochem.* **2011**, *80*, 301−325.
(9) Blanksby, S. J.; Mitchell, T. W. *Annu. Rev. Anal. Chem.* **2010**, *3*, 433−465.
(10) Hermansson, M.; Uphoff, A.; Käkelä, R.; Somerharju, P. *Anal. Chem.* **2005**, *77*, 2166−2175.
(11) Quehenberger, O.; Armando, A. M.; Brown, A. H.; Milne, S. B.; Myers, D. S.; Merrill, A. H.; Bandyopadhyay, S.; Jones, K. N.; Kelly, S.; Shaner, R. L.; Sullards, C. M.; Wang, E.; Murphy, R. C.; Barkley, R. M.; Leiker, T. J.; Raetz, C. R. H.; Guan, Z.; Laird, G. M.; Six, D. a.; Russell, D. W.; McDonald, J. G.; Subramaniam, S.; Fahy, E.; Dennis, E. a. *J. Lipid Res.* **2010**, *51*, 3299−3305.
(12) Ejsing, C. S.; Sampaio, J. L.; Surendranath, V.; Duchoslav, E.; Ekroos, K.; Klemm, R. W.; Simons, K.; Shevchenko, A. *Proc. Natl. Acad. Sci. U.S.A.* **2009**, *106*, 2136−2141.
(13) Klose, C.; Surma, M. a.; Gerl, M. J.; Meyenhofer, F.; Shevchenko, A.; Simons, K. *PLoS One* **2012**, *7*, e35063−e35063.
(14) Schwudke, D.; Oegema, J.; Burton, L.; Entchev, E.; Hannich, J. T.; Ejsing, C. S.; Kurzchalia, T.; Shevchenko, A. *Anal. Chem.* **2006**, *78*, 585−595.
(15) Bligh, E. G.; Dyer, W. J. *Can. J. Biochem. Physiol.* **1959**, *37*, 911−917.
(16) Folch, J.; Lees, M.; Sloane-Stanley, G. H. *J. Biol. Chem.* **1957**, *226*, 497−509.
(17) Matyash, V.; Liebisch, G.; Kurzchalia, T. V.; Shevchenko, A.; Schwudke, D. *J. Lipid Res.* **2008**, *49*, 1137−1146.
(18) Klemm, R. W.; Ejsing, C. S.; Surma, M. a.; Kaiser, H.-J.; Gerl, M. J.; Sampaio, J. L.; de Robillard, Q.; Ferguson, C.; Proszynski, T. J.; Shevchenko, A.; Simons, K. *J. Cell Biol.* **2009**, *185*, 601−612.

DOI: 10.1021/ac503627z
Anal. Chem. 2015, 87, 1749−1756

(19) Takamori, S.; Holt, M.; Stenius, K.; Lemke, E. a.; Grønborg, M.; Riedel, D.; Urlaub, H.; Schenck, S.; Brügger, B.; Ringler, P.; Müller, S. a.; Rammner, B.; Gräter, F.; Hub, J. S.; De Groot, B. L.; Mieskes, G.; Moriyama, Y.; Klingauf, J.; Grubmüller, H.; Heuser, J.; Wieland, F.; Jahn, R. *Cell* **2006**, *127*, 831−846.
(20) Ishida, Y.; Nakanishi, O.; Hirao, S.; Tsuge, S.; Urabe, J.; Sekino, T.; Nakanishi, M.; Kimoto, T.; Ohtani, H. *Anal. Chem.* **2003**, *75*, 4514−4518.
(21) Jackson, S. N.; Wang, H.-Y. J.; Woods, A. S. *Anal. Chem.* **2005**, *77*, 4523−4527.
(22) Passarelli, M. K.; Winograd, N. *Biochim. Biophys. Acta* **2011**, *1811*, 976−990.
(23) Sjövall, P.; Lausmaa, J.; Johansson, B. *Anal. Chem.* **2004**, *76*, 4271−4278.
(24) Touboul, D.; Kollmer, F.; Niehuis, E.; Brunelle, A.; Laprévote, O. *J. Am. Soc. Mass Spectrom.* **2005**, *16*, 1608−1618.
(25) Takáts, Z.; Wiseman, J. M.; Gologan, B.; Cooks, R. G. *Science (New York, N.Y.)* **2004**, *306*, 471−473.
(26) Wiseman, J. M.; Puolitaival, S. M.; Takáts, Z.; Cooks, R. G.; Caprioli, R. M. *Angew. Chem., Int. Ed. Engl.* **2005**, *44*, 7094−7097.
(27) Veloso, A.; Astigarraga, E.; Barreda-Gómez, G.; Manuel, I.; Ferrer, I.; Giralt, M. T.; Ochoa, B.; Fresnedo, O.; Rodríguez-Puertas, R.; Fernández, J. a. *J. Am. Soc. Mass Spectrom.* **2011**, *22*, 329−338.
(28) Lanekoff, I.; Thomas, M.; Laskin, J. *Anal. Chem.* **2014**, *86*, 1872−1880.
(29) Trede, D.; Schiffler, S.; Becker, M.; Wirtz, S.; Steinhorst, K.; Strehlow, J.; Aichler, M.; Kobarg, J. H.; Oetjen, J.; Dyatlov, A.; Heldmann, S.; Walch, A.; Thiele, H.; Maass, P.; Alexandrov, T. *Anal. Chem.* **2012**, *84*, 6079−6087.
(30) Berry, K. a. Z.; Li, B.; Reynolds, S. D.; Barkley, R. M.; Gijón, M. a.; Hankin, J. a.; Henson, P. M.; Murphy, R. C. *J. Lipid Res.* **2011**, *52*, 1551−1560.
(31) Anderson, D. M. G.; Ablonczy, Z.; Koutalos, Y.; Spraggins, J.; Crouch, R. K.; Caprioli, R. M.; Schey, K. L. *J. Am. Soc. Mass Spectrom.* **2014**, *25*, 1394−1403.
(32) Stauber, J. *Bioanalysis* **2012**, *4*, 2095−2098.
(33) Roach, P. J.; Laskin, J.; Laskin, A. *Analyst* **2010**, *135*, 2233−2236.
(34) Van Berkel, G. J.; Pasilis, S. P.; Ovchinnikova, O. *J. Mass Spectrom.* **2008**, *43*, 1161−1180.
(35) Kertesz, V.; Van Berkel, G. J. *J. Mass Spectrom.* **2010**, *45*, 252−260.
(36) Blatherwick, E. Q.; Van Berkel, G. J.; Pickup, K.; Johansson, M. K.; Beaudoin, M.-E.; Cole, R. O.; Day, J. M.; Iverson, S.; Wilson, I. D.; Scrivens, J. H.; Weston, D. J. *Xenobiotica* **2011**, *41*, 720−734.
(37) Stegemann, C.; Drozdov, I.; Shalhoub, J.; Humphries, J.; Ladroue, C.; Didangelos, A.; Baumert, M.; Allen, M.; Davies, A. H.; Monaco, C.; Smith, A.; Xu, Q.; Mayr, M. *Circ.: Cardiovasc. Genet.* **2011**, *4*, 232−242.
(38) Ejsing, C. S.; Duchoslav, E.; Sampaio, J.; Simons, K.; Bonner, R.; Thiele, C.; Ekroos, K.; Shevchenko, A. *Anal. Chem.* **2006**, *78*, 6202−6214.
(39) Zech, T.; Ejsing, C. S.; Gaus, K.; de Wet, B.; Shevchenko, A.; Simons, K.; Harder, T. *EMBO J.* **2009**, *28*, 466−476.
(40) Schroeder, M. J.; Shabanowitz, J.; Schwartz, J. C.; Hunt, D. F.; Coon, J. J. *Anal. Chem.* **2004**, *76*, 3590−3598.
(41) Husen, P.; Tarasov, K.; Katafiasz, M.; Sokol, E.; Vogt, J.; Baumgart, J.; Nitsch, R.; Ekroos, K.; Ejsing, C. S. *PLoS One* **2013**, *8*, e79736−e79736.
(42) Schuhmann, K.; Almeida, R.; Baumert, M.; Herzog, R.; Bornstein, S. R.; Shevchenko, A. *J. Mass Spectrom.* **2012**, *47*, 96−104.
(43) Han, X.; Yang, K.; Gross, R. W. *Rapid Commun. Mass Spectrom.* **2008**, *22*, 2115−2124.
(44) Chan, R. B.; Oliveira, T. G.; Cortes, E. P.; Honig, L. S.; Duff, K. E.; Small, S. a.; Wenk, M. R.; Shui, G.; Di Paolo, G. *J. Biol. Chem.* **2012**, *287*, 2678−2688.

DOI: 10.1021/ac503627z
Anal. Chem. 2015, 87, 1749−1756